Thermal Analysis of Enhanced Poly(vinyl alcohol)-Based Proton-Conducting Membranes Crosslinked with Sulfonation Agents for Direct Methanol Fuel Cells

J. M. Morancho, J.M. Salla, A. Cadenato, X. Fernández-Francos, P. Colomer, Y. Calventus, X. Ramis, R. Ruíz

Department Màquines i Motors Tèrmics, Universitat Politècnica Catalunya, Diagonal 647, 08028 Barcelona, Spain

ABSTRACT: Poly(vinyl alcohol)-based proton-conducting membranes, due to their high selectivity for water with respect to alcohols, have been suggested as a promising alternative to perfluorinated ionomer, Nafion®, widely used as an electrolyte in hydrogen (PEMFC) and direct methanol (DMFC) fuel cells. Sulfosuccinic acid (SSA) has been commonly used as a crosslinking agent to form an inter-crosslinked structure and a promoting sulfonating agent to enhance the ion conductivity. The introduction of SSA increases proton conductivity of PVA-based polymer electrolyte membranes and reduces methanol permeability. Crosslinking produces deep changes in the crystallinity of PVA membranes and also alters the state and content of water in the membrane. In addition, the presence of the protonic acid promotes the appearance of degradation reactions at temperatures well below those of unmodified PVA, thus producing a decrease in thermal and mechanical stability. In this work, the thermal and mechanical properties of membranes prepared using PVA with different proportions of SSA were investigated by calorimetry and mechanical thermal analysis. The results indicate that the crystallinity disappears in membranes containing 2% of SSA or more. As a result of the combined effect of the disappearance of crystallinity and the increase of crosslinking, the equilibrium water content first increases (up to 5% SSA) but at higher proportions of SSA it decreases. Above 100°C, the amorphous membranes undergo degradation reactions such as the elimination of lateral OH groups of PVA and the formation of polyene structures, making the membrane colored, brittle and crackly. © 2011 Wiley Periodicals, Inc. J Appl Polym Sci 124: E57–E65, 2012

Key words: poly(vinyl alcohol); membranes; differential scanning calorimetry (DSC); crystallization; thermal and chemical stability

INTRODUCTION

Poly(vinyl alcohol) [PVA] is a well-known, semicrystalline, low cost polymer with several interesting physical properties such as water solubility, biodegradability, biocompatibility, and nontoxicity. It possesses the capability to form hydrogels and membranes by chemical or physical methods. It has been widely used in a variety of fields such as the textile, cosmetics, and paper industry. It is also used in a variety of pharmaceutical and biomedical applications.[1–3]

Proton-exchange membrane fuel cells (PEMFCs) and direct methanol fuel cells (DMFCs), employing hydrogen and liquid methanol as a fuel, have been explored as the technology of choice for clean and efficient energy-conversion systems for automobiles, portable applications, and stationary power generation. The proton-exchange membrane (PEM) is a central and critical component in PEMFCs and DMFCs. As a result, there is much interest in the study and development of such membranes. The membrane must possess a suitable combination of properties: high proton conductivity, good mechanical and chemical stability, low permeability, limited swelling in the presence of water and fabrication costs appropriate for the application.[4,5]

The most commonly used and investigated membranes are of the perfluorinated type, of which Nafion® (DuPont) is the ubiquitous and best representative. In these membranes the ionic function is covalently attached to the polymer backbone and is most often a sulfonic acid group ($-SO_3H$).

In DMFCs applications, Nafion® membranes present, in addition to their high cost, a high osmotic drag, which makes water management at high current densities difficult and a high methanol crossover (methanol, crossing over from the anode side through the membrane to the cathode side, reacts with oxygen, produces heat, and reduces the energy-conversion efficiency).[6,7]
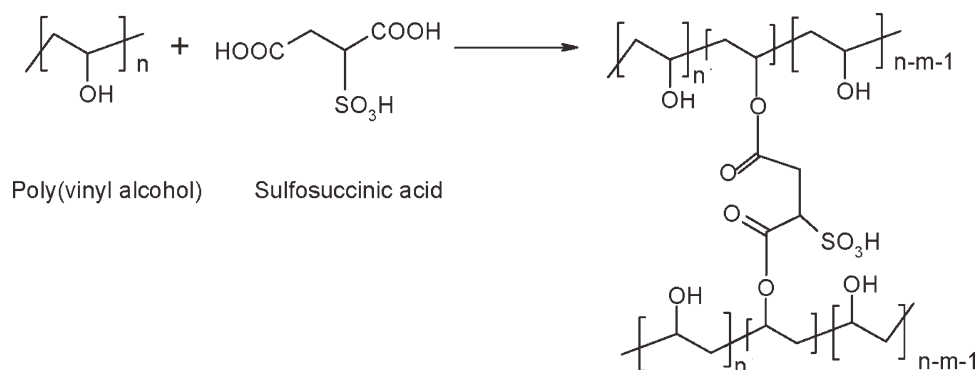
Scheme 1   PVA-SSA crosslinking reaction schema.

In recent years, there has been an intensive effort and a significant progress to develop a low-cost material suitable for DMFC membranes. Among them, poly(vinyl alcohol)-based proton-conducting membranes, due to their high selectivity for water with respect to alcohols and film-forming characteristics, has been suggested as a promising alternative. Sulfosuccinic acid (SSA) has been commonly used as a crosslinking agent to form an inter-crosslinked structure. Moreover SSA acts as sulfonating agent [8,9]. Scheme 1 shows the basic crosslinking reaction schema.

SSA, as a crosslinking agent, increases proton conductivity of PVA-based polymer electrolyte membranes and simultaneously reduces methanol permeability.[10] On the other hand, the crosslinking of PVA and the presence of protonic acid alter the mechanical and thermal behavior of the PVA-SSA membranes and their stability with respect to unmodified PVA ones.

The thermal and mechanical properties of pure PVA have been widely studied and referenced.[3,5,11–15] The presence of water acting as a plasticizer and the degree of crystallinity that may be greater than 50% give the PVA membrane excellent thermal and mechanical behavior. From the thermal point of view, pure PVA membranes begin to degrade above its melting temperature (220°C) and make it through two distinct processes. First the side OH groups are removed, releasing water and forming a polyene structure and afterwards, the main chains are broken and low molecular weight products are formed. In the case of PVA modified with agents to promote their proton conduction properties and their use as electrolyte in fuel cells, such as SSA, the reports found in the literature are mainly interested on the electrical properties, the permeability to different solvents and the formation of hydrogels. They show limited interest on thermal and mechanical properties because in many applications no great resistance is needed. In other cases, it is assumed that the compound will behave similar behavior to pure PVA. That is why this work, taking as a reference the properties of pure PVA, focuses on the analysis of physi-

cal and chemical changes produced by the inclusion of a protonic agent, SSA, and the changes that are subsequently produced in its thermal and mechanical behavior. First, using thermomechanical analysis, the elastic modulus of pure and compounded PVA was investigated as a function of temperature. DSC thermal analysis was used to analyze the changes on crystallinity and on the content and states of water. Finally, thermogravimetric analysis was performed to know the extent of thermal stability and degradability of pure PVA and PVA-SSA membranes.

EXPERIMENTAL

Materials

Poly(vinyl alcohol) (PVA, 99% hydrolyzed, average M_w: 89,000–98,000 g/mol) and sulfosuccinic acid, as the basic crosslinking agent (SSA, 70 wt % solution in water) from Aldrich were used as received.

Preparation of the materials

The membranes were prepared using a standard solution-cast method. PVA powders were dissolved in de-ionized water with continuous stirring at 90°C to form a 10 wt % PVA aqueous solution until a transparent solution was obtained. A given amount of SSA of a desired concentration was then added to this PVA solution and the mixture was stirred continuously until a homogeneous solution was obtained. The membranes were cast by pouring the solution onto Petri dishes and evaporating water under ambient conditions for 16 h. When visually dry, the membranes were peeled from the plastic substrate and had a thickness of about 0.3–0.1 mm.

CHARACTERIZATION AND MEASUREMENTS

Dynamic mechanical analysis

A dynamic mechanical analyzer (DMA Q800 V20 TA Instruments) was used for measuring the

temperature-dependant elastic moduli of the membranes investigated. Tests were conducted with single cantilever bending mode. The support span was 17.39 mm. The oscillation amplitude of displacement was kept at 15 μm. Specimens for DMA testing (10.3 mm x 13.3 mm x 0.21 mm) were cut from the selected membranes. The temperature profile ranged from 30°C to 150°C at a 3°C/min heating rate with a frequency of 1 Hz.

PVA melting behavior

The melting behavior of unmodified PVA membranes was analyzed with a Mettler DSC-822e calorimeter with a TSO801RO robotic arm. The calorimeter was calibrated using an indium standard (heat flow calibration) and an indium–lead–zinc standard (temperature calibration). Samples of ~ 5 mg in weight were put in covered aluminum pans. First, a nonisothermal run was performed between 20 and 250°C at a heating rate of 25°C/min, then the sample was cooled at 25°C/min to return at 20°C in order to impose a known thermal history. By means of a second heating scan between the same temperatures interval, the modified melting behavior was analyzed. Besides the melting peaks, the glass transition temperatures (T_g) were calculated as the temperature of the half-way point of the jump in the heat capacity in the cooling runs. We estimated the degree of crystallinity (x_c) using the following equation

$$x_c = \frac{\Delta h_c}{\Delta h_m^o} 100 \tag{1}$$

where Δh_m is the experimental enthalpy value through numerical integration of the area covered by the cooling peak and Δh_m^0 is the extrapolated enthalpy corresponding to the melting of a 100% crystalline sample. A value of 138.6 J g^{-1} for a theoretical 100% crystalline PVA was used according to Peppas et al.[16]

Freezing water and nonfreezing bound water

For a proton-conducting fuel cell membrane, the water uptake is a key issue to the fuel cell performances. The state of water is usually categorized into the following three different types: (a) free water, which shows the same temperature and enthalpy of melting/crystallization as bulk water; (b) freezing bound water, weakly bound to the ionic and polar groups in the polymer matrix, which exhibits a melting/crystallization temperature shifted with respect to that of bulk water but can be detected by melting transitions in DSC measurements, and (c) nonfreezing water, strongly bound to the ionic and polar parts of the polymer, which shows no detectable

phase transition over the range of temperatures normally associated with bulk water.[17,18]

Deionized water was sealed in a preweighed DSC aluminum pan. A final mass (water sample plus DSC pan) was taken and the mass difference between this and the empty DSC pan was recorded. The sealed pan was placed in a Mettler DSC-822e calorimeter, cooled to −40°C at a rate of 20°C/min and then heated to 40°C at a rate of 3°C/min.

PVA and PVA-SSA crosslinked samples were dried until a constant weight was achieved. The dried weight of the samples was recorded. The samples were full hydrated by immersing in deionized water at room temperature for more than 2 h. The weight of the full hydrated samples was also recorded after blotting with tissue paper to eliminate any liquid water adhered to the surface. The full hydrated samples were sealed in DSC aluminium pans and the same DSC runs as in the case of de-ionized water were performed. The enthalpy values were obtained by numerical integration of areas covered by the melting peaks and normalized by the water content mass. The onset and peak melting temperatures were also annotated. To calculate the bound water content (w_b), the normalized enthalpy values were compared with the normalized enthalpy of the pure water obtained, according to the following equation

$$w_b = m_{tw} \left(1 - \frac{\Delta h_m}{\Delta h_{m,H_2O}} \right) \tag{2}$$

where m_{tw} is the total water, Δh_m is the experimental enthalpy value through numerical integration of the area covered by the melting peak and $\Delta h_{m,H2O}$ is the experimental enthalpy of the melting peak of de-ionized water (330.2 J g^{-1}).

Stability analysis

The thermal stability of the membrane was evaluated using a thermogravimetric analyzer (Mettler TG50). The weight changes of the tested samples (10 mg) were recorded in a nitrogen gas flow (100 cm^3 min^{-1} measured in normal conditions) under a heating rate of 10°C min^{-1} from 40 to 500°C. Experimental integral curves were obtained and final remaining weight annotated. Normalized integral curves were derived using the usual procedure[19] and the degree of conversion of the mass loss was defined as:

$$\alpha = \frac{m_o - m}{m_o - m_\infty} \tag{3}$$

where m is the mass corresponding to a temperature T, m_o is the initial mass, and m_∞ is the mass of the substance at the end of the experiment. The rate of mass loss ($d\alpha/dt$) was also calculated.
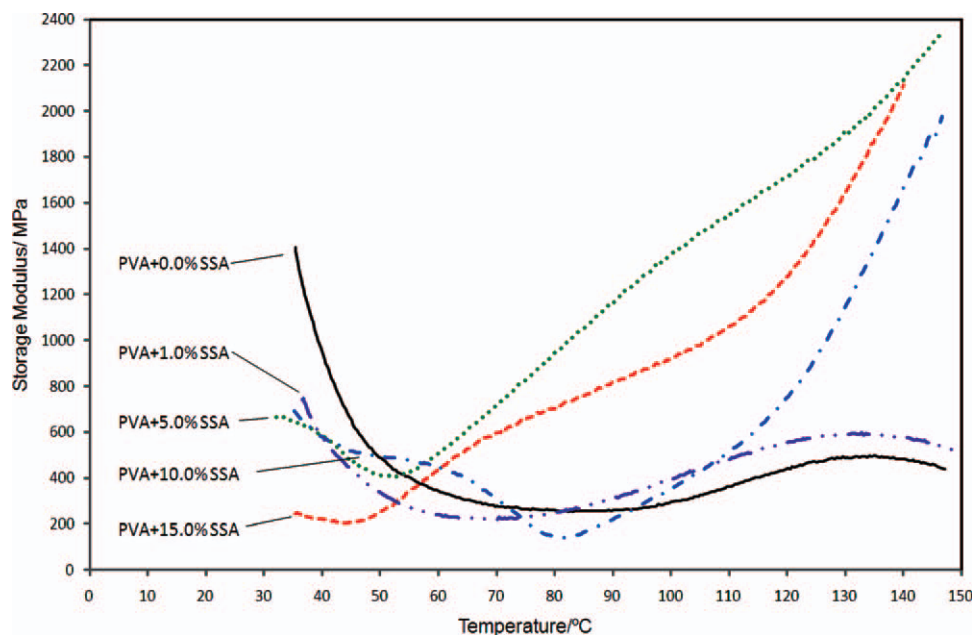
Figure 1 Temperature dependence of storage modulus (E') for PVA and PVA+SSA membranes. The measurements were conducted at a 3°C min^{-1} heating rate and 1-Hz frequency. [Color figure can be viewed in the online issue, which is available at wileyonlinelibrary.com.]

RESULTS AND DISCUSSION

Dynamic mechanical analysis

Figure 1 shows the temperature dependence of storage modulus (E') for PVA and PVA crosslinked membranes with different amounts of SSA. In Figure 1, the main relaxation process associated to glass transition is clearly seen as an important decrease of E', as the membranes move from unrelaxed state to a relaxed one. After the glass transition, an increase in the modulus can be observed because of water evaporation. Comparing the initial unrelaxed modulus of Figure 1, pure PVA membrane shows higher E' than PVA-SSA membranes, with a decreasing trend on increasing SSA content. Some factors may account to explain this behavior. One of them is the balance between the decrease of crystallinity and the increment of crosslinks. Many authors have studied the variation of the degree of crystallinity of pure PVA and blended or crosslinked PVA with different agents.[15,20–29] In most cases, the crosslinking produces a diminution of the degree of crystallinity. In our case, as it is reported in the next section, we obtained a degree of crystallinity of 51.5% for the unmodified PVA membranes, but no crystallinity was observed by DSC analysis for PVA membranes crosslinked with 2% of SSA or more. On the other hand, it is also known that the crosslinking increases the elastic modulus and the rigidity of the polymer.[20,21] Seeing the initial unrelaxed values of E', we must conclude that the mechanical stability that the crystalline structure gives to the membrane is

greater than the effect produced by the degree of crosslinking. The destruction of crystallinity is not compensated by the increment of crosslinks so pure PVA has the highest value of E'.

Another factor that must be taken into account is the water content. As it will be seen in the next sections, the introduction of SSA alters the content and the states of water equilibrium into the membrane. It is well known that water is an effective plasticizer for PVA.[18] The diminution of E' by increasing SSA content may be explained not only by water content but also the reduction of hydroxyl groups produced by the crosslinking. For pure PVA membranes it is reported[19] that the hydroxyl groups contribute via hydrogen bonding to the stiffness of the polymer. If the number of these groups is diminished by crosslinking, the hydrogen bonding is attenuated and the stiffness is diminished because the crosslinker induces less stiffness than the hydrogen bonding. The final mechanical behavior is a compromise between these effects: crystallinity, crosslink density and water content.

The effect of the crystalline content and temperature on the elastic modulus is better understood in Figure 2 where the normalized module $(E'-E'_o)/E'_o$, is plotted versus temperature (E'_o is the unrelaxed modulus). The evolution of E' in the crystalline samples is very different from the amorphous ones. In the crystalline membranes, E' first decreases as a consequence of the relaxation and then increases, because of water evaporation, goes through a maximum and later on gradually decreases up to the
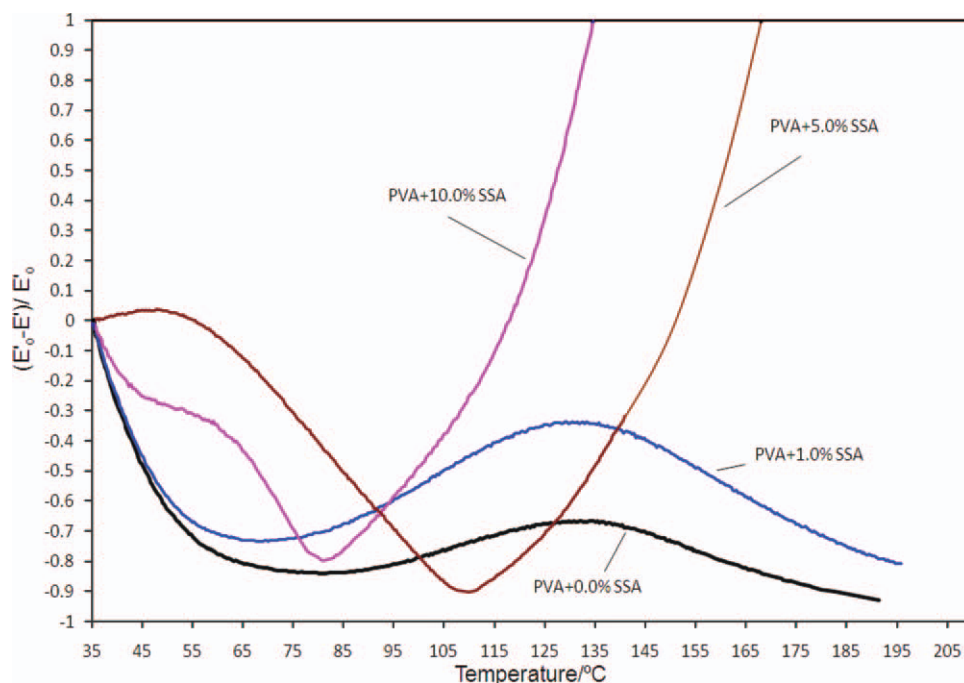
Figure 2 Temperature dependence of normalized storage modulus $[(E'-E'_o)/E'_o]$ for PVA and PVA-SSA membranes. [Color figure can be viewed in the online issue, which is available at wileyonlinelibrary.com.]

melting temperature. In the amorphous ones, after the initial drop, E' is continuously growing, reaching very high values. The high values of modulus of amorphous membranes, especially above 100°C, that Figures 1 and 2 show cannot only be attributed to the evaporation of free water. As it will be explained below, the chain-stripping elimination of water to form polyene structures as a first step of a degradation process may be the main cause.

PVA melting behavior

The DSC heating and cooling thermograms of pure PVA, 1 and 15% PVA+SSA membranes at a rate of 25°C min^{-1} are shown in Figure 3. In the heating curves, the first peak (at temperatures between 150 and 170°C) is associated to evaporation of water. In pure PVA and PVA+1% SSA, the second peak, above 220°C is associated to the melting of the
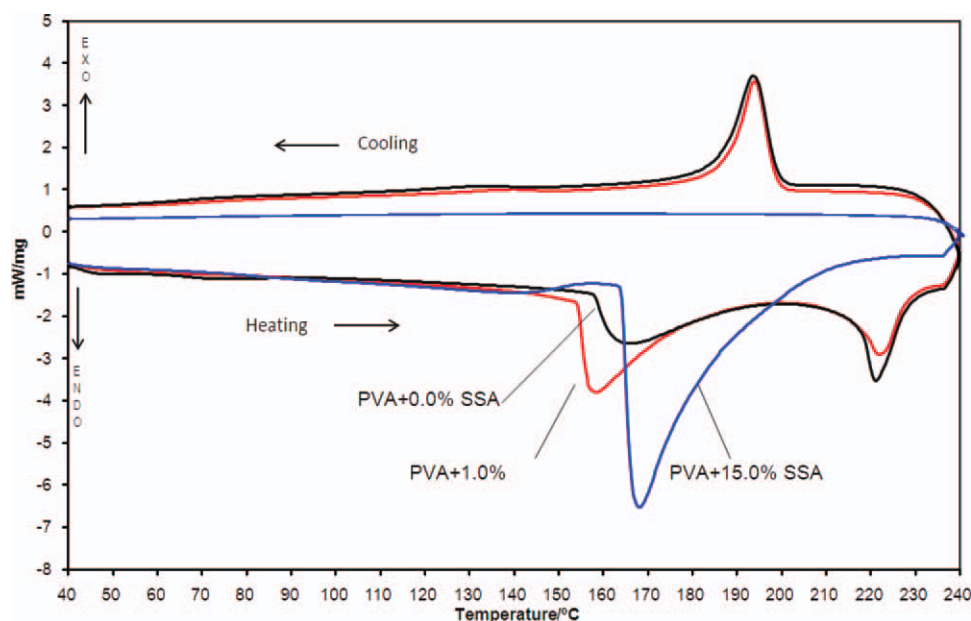

Figure 3 DSC heating and cooling thermograms of PVA and PVA-SSA membranes at 25°C min^{-1}. [Color figure can be viewed in the online issue, which is available at wileyonlinelibrary.com.]

TABLE I
Main Representative Parameters of Melting and Crystallization Peaks, Glass Transition Temperature, and Degree of Crystallinity of Pure PVA and PVA-SSA Membranes

Membrane	T_g (°C)[a]	T_m (°C)[b]	Δh_m (J/g)[c]	T_c (°C)[d]	Δh_c (J/g)[e]	x_c (%)[f]
PVA+0% SSA	64.5	221.2	44.9	193.7	69.7	51.5
PVA+1% SSA	72.8	221.7	39.0	193.8	58.6	46.3
PVA+15% SSA	82.1	–	–	–	–	–

[a] The glass transition temperature obtained from the cooling curve.
[b] The melting temperature (the temperature of melting peak).
[c] The experimental enthalpy value through numerical integration of area covered by the melting peak.
[d] The crystallization temperature (the temperature of cooling peak).
[e] The experimental enthalpy value through numerical integration of area covered by the cooling peak.
[f] Degree of crystallinity obtained from the cooling curve. A value of 138.6 J/g was used for PVA 100% crystalline.

membrane crystalline material. For these samples, in the cooling process, a crystallization peak appears. No melting/cooling appears for the PVA+15% PVA samples, so this membrane is amorphous. Table I shows the most representative parameters of melting and cooling peaks of Figure 3. In the crystalline samples, the difference between melting heat, Δh_m and cooling heat, Δh_c denotes the effect that the temperature cycle and the elimination of water produce on the crystallinity. The degree of crystallinity, x_c of Table III, obtained from cooling peak is higher than that would have been obtained by using the melting peak. On the other hand, the degree of crystallinity decreases in the sample PVA+ 1% SSA compared to pure PVA, as a consequence of crosslinks. This fact

is also reflected in the increase of T_g. The important changes that water content produces on crystallinity of pure PVA membranes and crosslinks using different PVA crosslinkers is a matter of great interest as it is reflected in the literature.[22–29]

Freezing water and nonfreezing bound water

Figure 4 shows the DSC heating thermograms of PVA-SSA crosslinked samples with different SSA content in the vicinity of 0°C, used to analyze the state of water in the crosslinked membranes, the bound and unbound (free and freezing) water. As a reference, the melting peak of deionized water is also added. It can be seen peaks with shoulder or
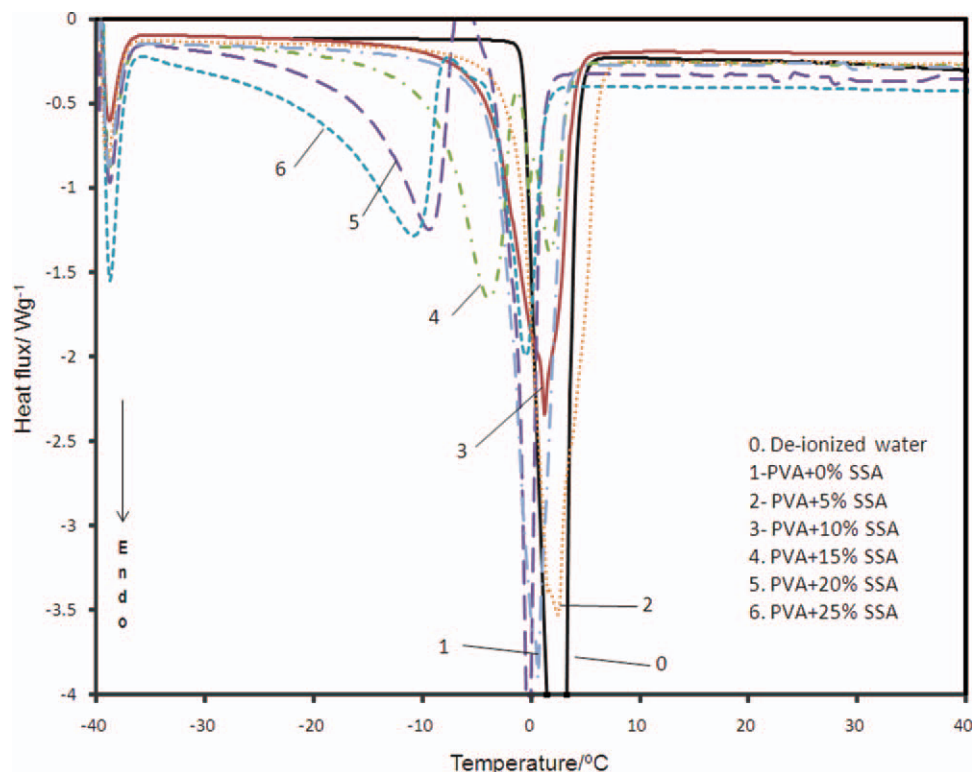

Figure 4 Melting curves of PVA-SSA crosslinked samples with different SSA content at the vicinity of 0°C. [Color figure can be viewed in the online issue, which is available at wileyonlinelibrary.com.]

TABLE II
The Distribution of Water States in Various PVA-SSA Crosslinked Membranes

Membrane	% SSA[a]	$g_{H2O}/g_{H2O,0\%}$[b]	Δh_m[c] (J/g_{H2O})	w_{ub}[d](%)	w_b[e](%)	w_b/w_{ub}	T_{1onset}[f] (°C)	T_{1p}[g] (°C)	T_{2onset}[h] (°C)	T_{2p}[i] (°C)
PVA+0% SSA	0	1.00	277.1	29.03	70.97	2.45	−3.0	0.6		
PVA+5% SSA	5	1.87	316.1	17.51	82.49	4.71	−1.1	2.5		
PVA+10% SSA	10	1.66	214.9	13.46	86.54	6.43	−1.3	1.3		
PVA+15% SSA	15	0.77	227.5	31.09	68.91	2.22	−9.0	−3.9	−0.3	1.8
PVA+20% SSA	20	0.32	245.8	84.96	15.04	0.18	−15.9	−9.4	−1.6	−0.3
PVA+25% SSA	25	0.29	243.1	91.74	8.26	0.09	−20.5	−10.9	−3.0	−0.6

[a] The composition of the formulations is given in weight %.
[b] Water/water of PVA+0% SSA membrane.
[c] Heat of melting peak around 0°C divided by mass of water.
[d] Unbound water/total water.
[e] Bound water/total water.
[f] Onset temperature of the first melting peak.
[g] Peak temperature of the first melting peak.
[h] Onset temperature of the second melting peak.
[i] Peak temperature of the second melting peak.

broad bimodal melting peaks depending on %SSA. It denotes the influence that crosslinks exert on the states of water. The sharp peak appearing near 0°C corresponds to the bulk-like free water and the broader peaks are due to the freezing bound water in the membranes. As mentioned earlier, the bound (w_b) (eq. 2) and unbound water content (w_{ub}), were computed from the total water content and the normalized enthalpy values of melting peaks of samples and deionized water.

The values of w_b, w_{ub} of samples investigated are shown in Table II, along with the variation of total water content of crosslinked membranes with respect to the unmodified PVA membrane. Table II also shows the ratio w_b/w_{ub} and the onset and peak temperatures of the melting peaks. It can be observed that, up to 10% SSA, samples have more water content than unmodified PVA. In membranes with 15% SSA or more, the water content is below the unmodified PVA value and it diminishes as SSA increases. The significant initial increase must be attributed to the decrease in crystallinity and the introduction into the membrane of hydrophilic groups (as –SO₃H), which compensates for the reduction of water provoked by the crosslinks. As SSA content increases, the reduction of water due the crosslinks prevails over the growing amount of hydrophilic ionic groups, thus decreasing the water content. It can be seen in Table II that, in membranes with 15% SSA or more, the ratio unbound water/total water considerably increases with SSA crosslinks while the ratio bound water/unbound water diminishes. As a result, the increment of crosslinks produces weak interactions between water and the polymer chains. This fact can be observed in the broad and bimodal melting peaks of Figure 4 and the onset and melting temperatures of Table II, which diminish as SSA increases.

According to the literature,[30,31] the strong association of the water to the ionomer reduces the electroosmotic drag of the water and methanol permeability, so membranes with a larger sorption of bound water compared with the unbound water (membranes with 10–15% of SSA) are the most suitable for using in DMFCs.

Stability analysis

The thermal degradation of polyvinyl alcohol (PVA) has been the subject of several studies with thermal analysis.[32,33] It was found that pure PVA thermally degrades in two steps. The first degradation step takes place between 130 and 260°C and mainly involves elimination of side groups from the main chain and the loss of water. As a consequence, a growing number of unsaturations appear in the main chain, which progressively turns into a polyene structure. The second degradation process is dominated by chain-scission and cyclization reactions. The presence of acidic compounds can promote and accelerate these elimination reactions by protonating OH groups.[33]

The experimental TGA analysis of unmodified PVA and PVA-SSA membranes reveals a very different stability. The rate of mass loss ($d\alpha/dt$) of unmodified PVA and PVA-SSA crosslinked membranes, with respect to temperature, is shown in Figure 5. Table III shows the most representative parameters of the weight loss. Two separate steps, room temperature-220°C and 220–400°C can be observed. For the pure PVA, the small weight loss of the first step can be exclusively associated to water evaporation (7.6%). The degradation of PVA (chain-stripping elimination of water to form polyene, followed by breakage of the main chain)
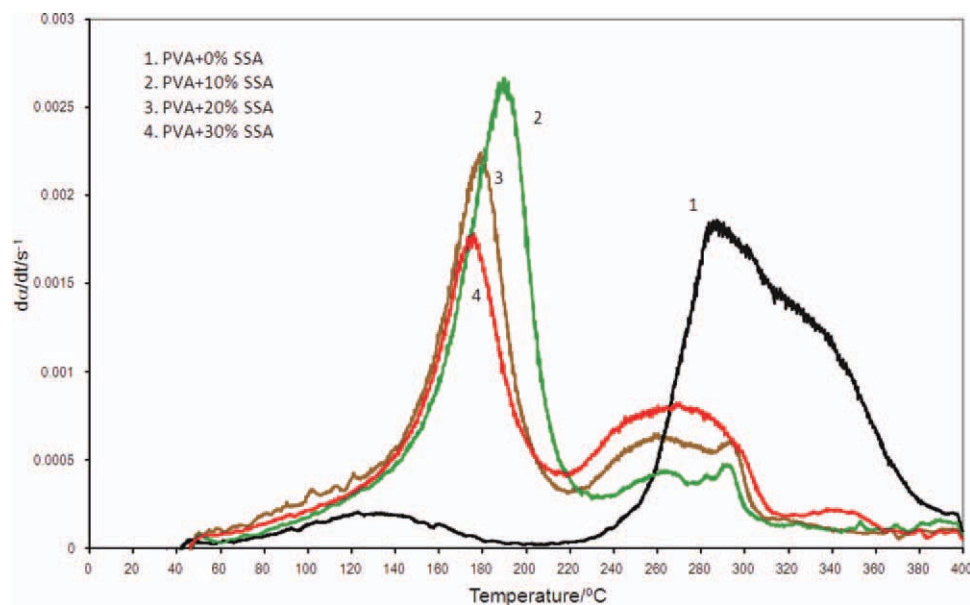
Figure 5 The evolution with temperature of the rate of mass loss ($d\alpha/dt$) of unmodified PVA and PVA-SSA crosslinked membranes. [Color figure can be viewed in the online issue, which is available at wileyonlinelibrary.com.]

takes place between 250–400°C. At 400°C the yield char is 20%.

In PVA-SSA membranes there is no separation between the peaks of the evaporation of water and the first degradation process. At the end of the step, the weight loss hardly depends on the SSA content. The possible increase of the stability produced by the crosslinking degree is counterbalanced by the elimination reactions. It is noteworthy that these reactions in the PVA-SSA samples are produced at very low temperatures compared to the unmodified PVA ones. Above 80°C, PVA-SSA membranes suffer some degree of darkening indicating that these degradation reactions are produced to some extent. The advance of thermal degradation of PVA-SSA membranes with respect to pure PVA may be caused by the acceleration produced by the acidic environment of the sulfonate groups added by SSA.[34] This fact is also observed in Figure 5 with the advance of the

DTG peaks when the SSA content increases. It also explains the high increment that temperature produces in the elastic modulus of amorphous membranes and the fact that membranes become brittle and cracky.

The second degradation step of PVA-SSA membranes appears at lower temperatures than pure PVA. The char residue varies between 40.9–51.9% of the initial weight.

CONCLUSIONS

As far as the thermal and mechanical properties are concerned, the crosslinking of PVA with SSA produces important changes with respect to the unmodified PVA membranes due to the variation of the degree of crystallization and the equilibrium water content. The proportion of SSA and the

TABLE III
Thermogravimetric Data of the Two Main Processes of Membranes with Different SSA Content, Obtained from Experimental DTGA Curves at 10°C/min

Membrane	% SSA[a]	40–220°C process		220–400°C process	
		T_{P1}[b](°C)	α_{200}[c](%)	T_{P2}[d](°C)	Char yield[e](%)
PVA+0% SSA	0	287.5	7.6	340.0	20.0
PVA+10% SSA	10	189.3	30.9	289.7	51.9
PVA+20% SSA	20	178.5	33.2	290.3	46.6
PVA+30% SSA	30	176.0	30.8	274.2	40.9

[a] The composition of the formulations is given in weight %.
[b] Temperatures of the peak in the DTG signal, 40–220°C interval.
[c] % mass volatilized until $T = 220$°C.
[d] Temperatures of the peak in the DTG signal, 220–400°C interval.
[e] % residual mass at 400°C (char yield).

thermal treatment also affect the characteristics of the water into membrane (nonfreezing bound water, weakly bound water, and free water).

The acidity of SSA modifies the thermal stability of PVA-SSA membranes via water elimination reactions and chain breakage at very low temperatures. This fact is not compensated with the increment of crosslinking degree produced when SSA content is increased.

To enhance the behavior of poly(vinyl alcohol) based proton conducting membranes it is necessary to avoid excessive alteration of the degree of crystallization and to control the acidity of the medium to prevent water elimination reactions when membranes are fabricated.

References

1. Hassan, C. M.; Peppas, N. A. Adv Polym Sci 2000, 153, 37.
2. Da silva, E.; Lebrun, L.; Metayer, M. Polymer 2002, 43, 5311.
3. Kobayashi, M.; Toguchida, J.; Oka, M. Biomaterials 2003, 24, 639.
4. Neburchilov, V.; Martin, J.; Wang, H.; Zhang, J. J Power Sources 2007, 169, 221.
5. Bayrakçeken, A.; Erkan, S.; Türker, L.; Eroglu, I. Int J Hydrogen Energy 2008, 33, 165.
6. Mauritz, K. A.; Moore, R. B. Chem Rev 2004, 104, 4335.
7. Nam, S.-E.; Kim, S.-O.; Kang, Y.; Lee, J. W.; Lee, K-H. J Membrane Sci 2008, 322, 466.
8. Hirankumar, G.; Selvasekarapandian, S.; Kuwata, N.; Kawamura, J.; Hattori, T. J Power Sources 2005, 144, 262.
9. Rhim, J.-W.; Park, H. B.; Lee, C.-S.; Jun, J.-H.; Kim, D. S.; Lee, Y. M. J Membr Sci 2004, 238, 143.
10. Tsai, C. E.; Lin, C. W.; Hwang, B. J. J Power Sources 2010, 195, 2166.
11. Herrera-Kao, W.; Aguilar-Vega, M. Polym Bull 1999, 42, 449.
12. Kreuer, K. D. J Membr Sci 2001, 85, 29.
13. Cascone, M. G. Polym Int 1997, 43, 55.
14. Park, J.-S.; Park, J.-W.; Ruckenstein, E. J Appl Polym Sci 2001, 82, 1816.
15. Hassan, C. M.; Peppas, N. A. Macromolecules 2000, 33, 2472.
16. Peppas, N. A.; Merrill, E. W. J Polym Sci Polym Chem 1976, 14, 441.
17. Gohil, J. M.; Bhattacharya, A.; Ray, P. J Polym Res 2006, 13, 161.
18. Lue, S. J.; Shieh, S. J. Polymer 2009, 50, 654.
19. Arasa, M.; Ramis, X.; Salla, J. M.; Mantecon, A.; Serra, A. Polym Degrad Stabil 2007, 92, 2214.
20. Peng, Z.; Chen, D. J Polym Sci Part B: Polym Phys 2006, 44, 534.
21. Shen, C.-C.; Joseph, J.; Lin, Y.-C.; Lin, S.-H.; Lin, C.-W.; Hwang, B. J. Desalination 2008, 233, 82.
22. Oda, S.; Tanaka, J. I.; Ohta, H. J Fermentation Bioeng 1998, 86, 84.
23. Gimenez, V.; Mantecon, A.; Cadiz, V. J Polym Sci Part A 1996, 34, 925.
24. Probst, O.; Moore, E. M.; Resasco, D. E.; Grady, B. P. Polymer 2004, 45, 4437.
25. Stasko, J.; Kalninš, M.; Dzene, A.; Tupureina, V. Proc Estonian Acad Sci 2009, 58, 63.
26. Wong, S.-S.; Altinkaya, A.-S.; Mallapragada, S.-K. J Polym Sci Part B: Polym Phys 2007, 45, 930.
27. Huang, H.; Gu, L.; Ozaki, Y. Polymer 22, 47, 3935.
28. Lee, J.; Lee, K.-J.; Jang, J. Polym Test 2008, 27, 360.
29. Li, L.; Chen, N.; Wang, Q. J Polym Sci Part B: Polym Phys 2010, 48, 1946.
30. Huang, Y. F.; Chuang, L. C.; Kannan, A. M.; Lin, C. W. J Power Sources 2009, 186, 22.
31. Wang, T.; Gunasekaran, S. J Appl Polym Sci 2006, 101, 3227.
32. Gilman, J. W.; VanderHart, D. L.; Kashiwagi, T. In Fire and Polymers II: Materials and Tests for Hazard Prevention; Nelson GL, editor. American Chemical Society: Washington DC, 1994, p 161.
33. Holland, B. J.; Hay, J. N. Polymer 2001, 42, 6775.
34. Alexy, P.; Káchová, D.; Krsiak, M.; Bakos, D.; Simkova, B. Polymer Degrad Stabil 2002, 78, 413.